

Metal-enhanced fluorescence based excitation volumetric effect of plasmon-enhanced singlet oxygen and super oxide generation

Cite this: *Phys. Chem. Chem. Phys.*, 2013, **15**, 15740

Jan Karolin and Chris D. Geddes*

In this contribution we show that the Metal-Enhanced Fluorescence (MEF) Excitation Volumetric Effect (EVE), has a profound effect on the formation of Reactive Oxygen Species (ROS), such as singlet oxygen ($^1\text{O}_2$) and superoxide anion radical ($\text{O}_2^{\cdot-}$), when sensitizers are placed in close proximity to plasmon supporting nanoparticulate substrates. In particular, when the singlet oxygen sensitizer rose bengal is placed on a SiFs surface, *i.e.* on a silver island film, the $^1\text{O}_2$ response to power is non-linear, and at 100 mW excitation power (535 nm) it is about 5 times higher, as compared to glass control samples, measured with the commercially available $^1\text{O}_2$ probe Sensor Green™. We also report a similar power dependence of superoxide generation for acridine on SiFs surfaces, but using the dihydroethidium $\text{O}_2^{\cdot-}$ probe (DHE). Our findings are consistent with our previously postulated Metal-Enhanced Fluorescence (MEF) and EVE models.

Received 3rd March 2013,
Accepted 10th July 2013

DOI: 10.1039/c3cp50950h

www.rsc.org/pccp

Introduction

Metal-Enhanced Fluorescence (MEF),¹ *i.e.* increasing the fluorescence signature of fluorophores close to metallic nanoparticles, has rapidly become an important field of study, both from a mechanistic/theoretical perspective, as well as for the development of new ultra-sensitive biological assays.^{2–6} The effect has its origins in the optical near-field coupling between metallic nanoparticles and fluorophores; a coupled system with a high density of states and a high degree of both ground and excited state wave-functional overlap ($\Psi \rightarrow \Psi^*$), with subsequent benefits on triplet yields,⁷ excimer emission,⁸ and e-type fluorescence.⁹ Metal-enhanced triplet yield, or metal enhanced phosphorescence, MEP, has been demonstrated by observing the enhanced formation of reactive oxygen species (ROS), such as singlet oxygen and superoxide, for sensitizers close to metallic nanoparticles.^{10–12}

In a previous publication by Zhang *et al.*¹³ the plasmon enhanced generation of singlet oxygen was investigated under constant illumination power, but for sensitizers at various distances from Ag particles as adjusted by the thickness of vacuum deposited SiO_2 coatings. A correlation between the singlet oxygen generation efficiency and the electromagnetic field

strengths, simulated by the finite-difference time-domain (FDTD) technique, was reported, and further, using different sensitizers it was found that the extent of singlet oxygen enhancement is inversely proportional to the free space singlet oxygen quantum yield. In the present report we investigate how the illumination power influences the formation of ROS, and in particular, we report a non-linear relationship that well correlates with the Excitation Volumetric Effect (EVE), previously reported by Geddes.¹⁴

For MEF EVE, a modulation in MEF efficiency is observed as a function of far-field ($>1\lambda$ light away) excitation irradiance,¹³ which can readily be explained by the near-field electric field volume around nanoparticles, increasing non-linearly with increasing far-field excitation power.¹³ Subsequently, fluorescence intensity increases non-linearly while the amplitude weighted lifetime of a heterogeneous sample decreases as a function of increased excitation power.¹⁵

The probe used to detect singlet oxygen in the present work is the commercially available Sensor Green® (Invitrogen, USA). The probe is reported to be highly selective for singlet oxygen and is water soluble at mM concentrations. The structure of Sensor Green has not been released by Invitrogen, but has been speculated to be a bichromophoric molecule in a so-called PET (photoinduced electron transfer) design, consisting of an anthracene moiety attached to a fluorescein unit,^{16,17} Fig. 1A. An efficient photoelectron transfer process quenches the fluorescein emission; however, in the presence of singlet oxygen anthracene forms an endoperoxide SOSG-EP disrupting the conjugated

Institute of Fluorescence and Department of Chemistry & Biochemistry, The Columbus Center, University of Maryland Baltimore County, 701 East Pratt Street, Baltimore, MD 21202, USA. E-mail: jan.karolin@gmail.com, chrisgeddes72@gmail.com, geddes@umbc.edu; Fax: +1-410-576-5722; Tel: +1-410-576-5723

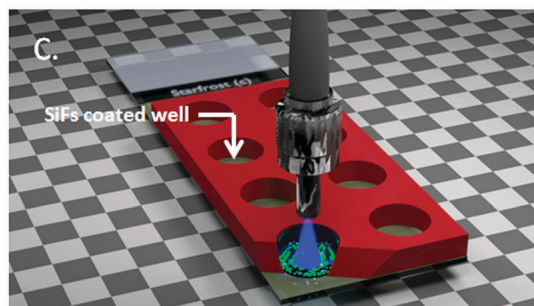
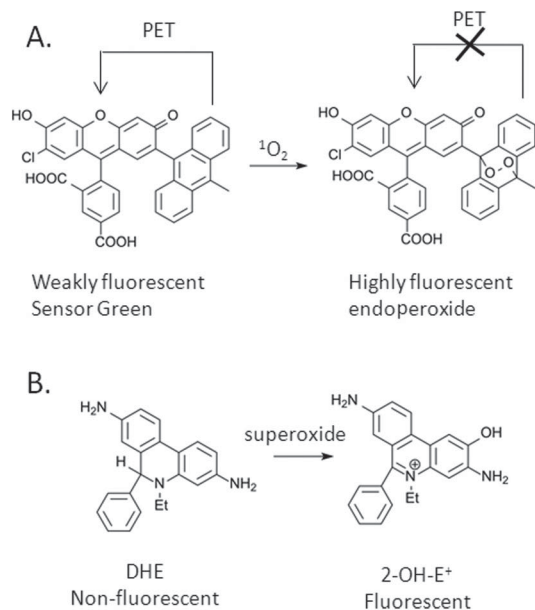


Fig. 1 (A) Oxidation of Sensor Green. The photoinduced electron transfer (PET) process quenches the emission from the fluorescein unit in Sensor Green. In the presence of singlet oxygen the anthracene chromophore reacts to form an endoperoxide and the PET mechanism is switched off, resulting in an increase in fluorescence intensity. (B) Oxidation of DHE. DHE is non-fluorescent but is oxidised in the presence of superoxide to an fluorescent ethidium cation. (C) Cartoon of the experimental detection of metal-enhanced ROS.

system allowing fluorescein to relax *via* fluorescence emission route. The reaction is irreversible, and the fluorescein signal is proportional to the singlet oxygen concentration in the solution.

To detect superoxide we have used the dihydroethidium (DHE) probe, also referred to as hydroethidium (HE). The probe has been used in numerous publications to detect superoxide generation, both in intracellular environments^{18–20} and in the vascular system,²¹ but its selectivity has recently been questioned.²² In the presence of superoxide the DHE probe reacts to form a 2-hydroxyethidium cation (2-OH-E⁺),^{23,24} Fig. 1B, that shows a characteristic fluorescence band centred around 586 nm when excited at 473 nm. The oxidation of DHE is an irreversible process and the fluorescent signal is proportional to the concentration superoxide in the solution.

Experimental

Materials

Silane-prep glass microscope slides, silver nitrate (99.9%), sodium hydroxide (99.996%), ammonium hydroxide (90%), D-glucose, ethanol (HPLC/spectrophotometric grade), anhydrous glycerol were purchased from Sigma-Aldrich (Milwaukee, WI, USA). Rose bengal and acridine were purchased from Sigma-Aldrich and the probes Singlet Oxygen Sensor Green[®] (SOSG) and dihydroethidium (DHE) were purchased from Invitrogen (Grand Island, NY, USA). The synthesis of SiFs was according to previously published procedures.^{25–29} Briefly, sodium hydroxide was added to a 60 ml cold solution of AgNO₃. The resulting precipitate of Ag₂O was dissolved by adding NH₄OH whereby a silver amine complex is formed, *e.g.* Ag(NH₃)₂⁺, that subsequently is reduced to Ag(s) particles by the addition of glucose.

The Ag(s) particles are deposited on amino-coated glass microscope slides (Silane-Prep, Sigma) that are immersed in the solution. The density of the Ag nanoparticles is controlled by altering both the deposition time, heat and reactant concentration, which can readily be measured from the absorption spectra.

Sample preparation and measurements

The singlet oxygen and superoxide generation on glass and SiFs surfaces was measured from press-to-seal silicon isolator wells (12 wells per slide), Fig. 1C. The silicon isolator was positioned so that 6 of the wells were on a SiFs surface and 6 on a clean SiO₂ area, the latter wells were used for reference measurements where no surface enhanced phenomena are possible, enabling the benefits of the SiFs plasmon enhancement to be realized. For each recording at a specific excitation power a total of 3 + 3 readings were measured, sensitizer + probe, probe alone, and the sensitizer alone. The enhancement factor for the reactive oxygen species were then calculated as outlined in the data analysis section.

The volume solvent added to each well was 25 μl, and the fill height thus approximately 0.5 mm. Care was taken to focus the laser used to excite the sensitizers, *i.e.* λ_{exc} = 266 nm or 532 nm, to fill the clear aperture (~4 mm) of the silicon well, giving a homogeneous distribution of oxidised probe molecules across the well surface. The excitation power was adjusted by a continuous variable neutral density filter wheel (Edmunds Optics).

Sensor Green[®] was purchased in vials and kept frozen at –20 °C until used, when 33 μl of methanol was added. In all prepared samples, except that for the blank solution, the concentration Sensor Green was 5 μM and rose bengal 10 μM. Because of the limited solubility of rose bengal in water a volume fraction of 15% methanol was left in the solutions.

Samples for the superoxide generation were prepared in a similar way, but due to the low solubility of acridine and DHE in water, spectroscopic methanol was used as the solvent. The concentration of DHE was ~ 0.5 mM and the acridine concentration $50 \mu\text{M}$.

Rose bengal was excited through a fiber optic coupled CW laser from Lasermate Group INC, USA, centred at 532 nm. A 266 nm laser, QUVL266-20 from Laser Lab Components, Inc., USA, was used to pump acridine, however this laser was not fiber optic coupled, but focused directly on the sample surface. The illumination time was controlled by a mechanical shutter mechanism. The power was measured at the position of the sample surface using a power meter, THORLABS PM100D, USA, with a S120VC detector. Immediately after pumping the sensitizer the signal from the probe molecule was measured, $\lambda_{\text{ex}} = 473$ nm, through a $400 \mu\text{m}$ bifurcated optical fiber from OceanOptics, USA. To suppress contamination from scattered excitation light a 473 nm StopLine[®] single-notch filter from Semrock, USA, was inserted in the beam path and the fluorescence signal was subsequently recorded on an OceanOptics spectrograph HR2000+. The spectra was analysed in SpectraSuite software.

Data analysis

For calculating the enhancement factor for singlet oxygen or superoxide generation, corrections must be made for the *inherent* enhanced emission observed from the probe molecules on the SiFs surface. In this work we follow the correction protocol outlined by our group, Zhang *et al.*,¹³ briefly; the metal enhanced fluorescence factor, α , for a fluorophore on a SiFs surface is defined as

$$\alpha = \frac{\int I_{\text{SiFs}}(\lambda) d\lambda}{\int I_{\text{SiO}_2}(\lambda) d\lambda} \quad (1)$$

where I indicates the fluorescence spectra recorded as function of wavelength on SiFs and on a glass substrate. The enhancement factor was typically found to be 3.3 and 2.1 for Sensor Green and DHE, respectively. In the case of Sensor Green an additional background correction must be introduced for the rose bengal signal as the emission bands overlaps. The full

expression for the enhanced singlet oxygen generation, $^1\text{O}_{2,\text{MEF}}$, is subsequently;

$$^1\text{O}_{2,\text{MEF}} = \frac{\int I_{\text{SiFs}}^{\text{SOG+RB}}(\lambda) d\lambda - \int I_{\text{SiFs}}^{\text{RB}}(\lambda) d\lambda}{\alpha \left[\int I_{\text{SiO}_2}^{\text{SOG+RB}}(\lambda) d\lambda - \int I_{\text{SiO}_2}^{\text{RB}} d\lambda \right]} \quad (2)$$

where $I(\lambda)$ indicates the emission intensity at wavelength λ . The subscripts, *i.e.* SiFs or SiO₂, indicate the substrate and the superscript indicates the sample composition, *e.g.* SOG + RB is the mixture of Sensor Green with the sensitizer rose bengal.

Results and discussion

The UV-Vis absorption spectra recorded for a typical SiFs is shown in Fig. 2A. The magnitude and shape of the absorbance band is a function of the chemical deposition time, *i.e.* to the density of silver islands on the glass surface, and to the particle geometry.²⁹ For a dry SiFs the absorption peak maxima is centred around 390 nm, while for a water immersed SiFs, the peak is broadened and shifted towards longer wavelengths ~ 440 nm. This correlates well with silver nanoparticles synthesised in colloidal solution, *e.g.* Evanoff *et al.*³⁰ reports a plasmon peak absorbance maxima close to 440 nm for 60 nm silver nanoparticles dispersed in water. The advantage of using SiFs surfaces for MEF applications, as compared to colloidal solutions, is the very high particle density that can be achieved on a surface.

In Fig. 2B the synchronous spectra is shown for a typical SiFs surface. In a synchronous spectra the excitation and emission wavelength are scanned simultaneously, *i.e.* $\lambda_{\text{ex}} = \lambda_{\text{em}}$, and the recorded spectra thus contains information about the scattering properties of the surface. Dragan *et al.*³¹ reported that the synchronous spectra correlates well with the wavelength dependence of MEF,³⁰ and can be used as a predictor of MEF. It is thus interesting to notice that the sensitizers used for the generation singlet oxygen in the present work, *i.e.* rose bengal, overlap well with the synchronous spectra as shown in Fig. 2B. We have observed a typical 2.5 times enhancement of the emission intensity detected from rose bengal on a SiFs surface, as compared to rose bengal on a glass surface, *i.e.* the control sample.³²

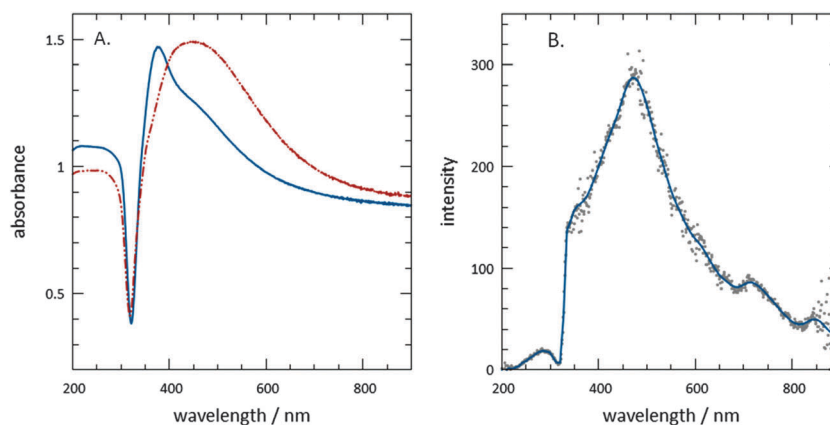


Fig. 2 (A) Absorption spectra recorded from dry SiFs (blue solid line) and on the same SiFs immersed in water (red dotted line). Note that spectra shown here are recorded from SiFs prepared on a quartz slide. (B) The synchronous spectra recorded on the dry SiFs is shown in part (A).

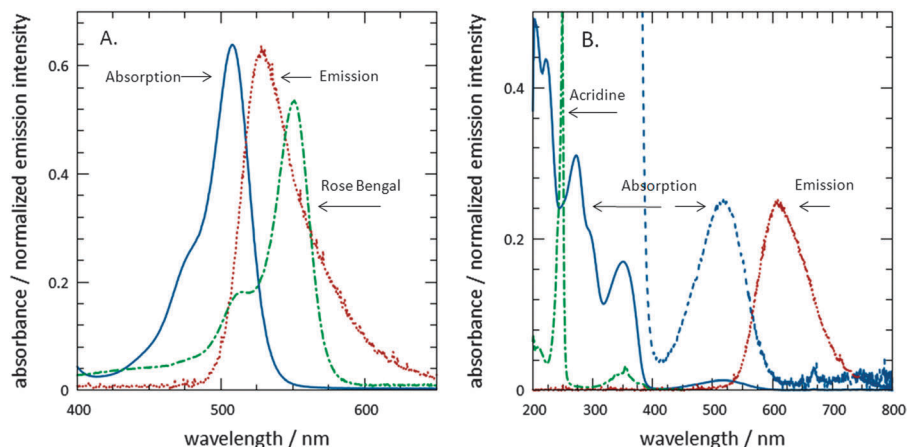


Fig. 3 Absorption and emission spectra recorded for (A) Sensor Green[®] (sg) and (B) the dihydroethidium probe (DHE). The absorption spectra for the sensitizers rose bengal and acridine are shown for comparison.

It can further be observed from the synchronous spectra that a small band is present around 250 nm, Fig. 2B. Although the nature of this band is not fully understood, it is noted that there is spectral overlap with the absorption spectra of acridine. The excitation wavelength for acridine was thus chosen to be 266 nm.

The absorption and emission spectra recorded for the probe molecules Sensor Green[®] and dihydroethidium are shown in Fig. 3. The recorded emission spectra for Sensor Green, excitation at 473 nm, is very similar to that observed for fluorescein and a far-field MEF factor close to 3 is commonly observed. This correlates well with a previous observation of MEF of fluorescein on a similar silver surface where a MEF of ~ 4.5 was reported.³¹ The dihydroethidium fluorophore emission is very weak when excited at 473, however, oxidised by superoxide a 2-hydroxyethidium (2-OH-E⁺) species is formed that shows a strong fluorescence centred at 586 nm.^{23,24} The emission spectra recorded for 2-OH-E⁺ in the present work is slightly red shifted, Fig. 3B. This is likely explained by the choice of solvent, methanol in the present case, and further, the spectra were recorded from a SiFs surfaces.

The striking power dependence of singlet oxygen generation can also be *visually* seen from the SiFs surface, Fig. 4. Here a mixture of Sensor Green and rose bengal are localised in SiFs wells as well as on glass surfaces, *i.e.* the reference samples, and

illuminated for 15 seconds at different excitation powers at 532 nm. The autogeneration of singlet oxygen by the probe molecule Sensor Green without the sensitizer rose bengal present are also shown. Although a weak fluorescence can be observed it is very small as compared to the sample.

The third-order nonlinear susceptibility for Ag nanoparticles on glass slides has previously been reported to be amplified 10^4 times close to the plasmon resonance band.^{33,34} The power dependence of the MEF factor for silver plasmon coupled fluorophores was reported by Dragan and Geddes¹⁴ to be strongly nonlinear. The phenomenon is referred to as the excitation volumetric effect, EVE, and a further correlation with the shortening of the fluorescence lifetime has also been reported.¹⁵ In the presence study it was thus deemed interesting to investigate the dependence of the sensitized generation of reactive oxygen species as function of excitation power on a SiFs surface. In Fig. 5A we show the calculated enhancement factor for singlet oxygen generation and in Fig. 5B that for superoxide. It is observed that the enhancement factor for singlet oxygen increase ~ 4 times as the excitation power is increased from 4 mW to 60 mW at 532 nm, and that the increase is nonlinear with excitation power. This observation correlates well with the excitation volumetric effect.¹⁴ The power dependence of the superoxide generation

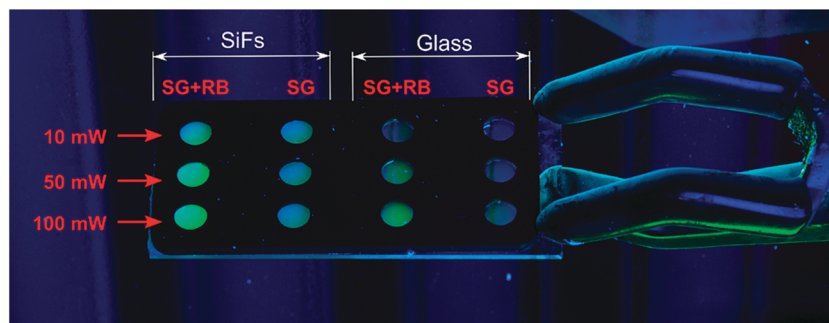


Fig. 4 Real color photograph showing a microscope slide with attached silicon isolators. Half of the microscope slide was coated with SiFs and the remaining half uncoated and used as a control sample. The photograph shows the visual effect of an increased laser power on near-field ¹O₂ generation. SG and RB refers to Sensor Green and rose bengal, respectively.

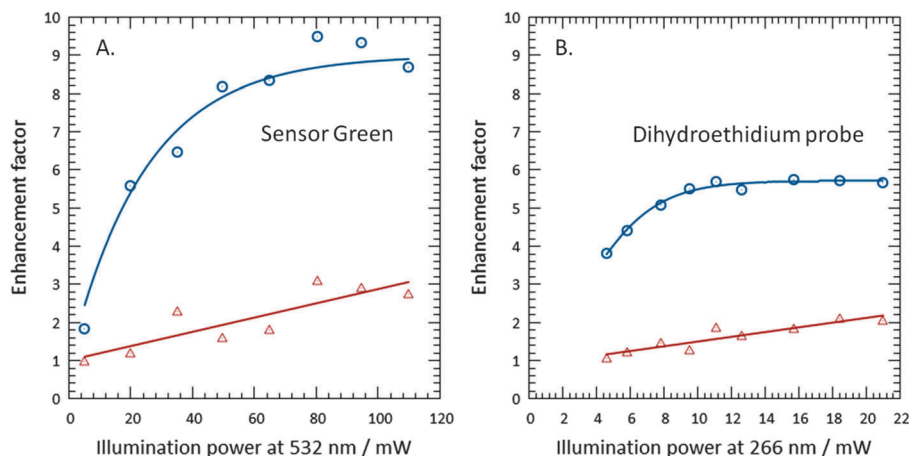


Fig. 5 (A) The enhancement factor for singlet oxygen generation in the presence (circles) and absence of rose bengal (triangles). (B) The enhancement factor for superoxide generation in the presence (circles) and absence of acridine (triangles).

on SiFs is not as pronounced as in the singlet oxygen case. However, increasing the excitation power from 4 mW to 10 mW at 266 nm causes a 1.5 times increase in the superoxide generation efficiency. The lower enhancement factor observed for superoxide generation correlates with the synchronous spectra as shown in Fig. 2B. The smaller overlap integral with the acridine spectra in the UV region, below 300 nm, is predicted to cause a smaller MEF.³¹

The plateau values observed in Fig. 3 likely reflects a depletion of probe molecules, *i.e.* Sensor Green or dihydroethidium, in the excitation region and/or that the available oxygen dissolved in the reaction mixture has oxidised.

Conclusions

In this work we have shown that the sensitizing molecules Sensor Green and acridine couples with surface plasmon on SiFs surfaces and that the generation of reactive oxygen species depends non-linearly on the excitation power. We have also shown that the enhancement factor for reactive oxygen species correlates with the synchronous spectra recorded for SiFs surfaces. Interestingly, our results support strongly the recent MEF EVE postulate,¹³ and further a recent report on how fluorophore-plasmon coupled luminescence lifetimes are also a function of far-field excitation irradiance.³⁴ In terms of life science applications, our results suggest that one can readily tune the extent of ROS generation in a system by simply tuning the excitation power irradiance on a sample. While the ROS probes are non-reversibly destroyed in the detection protocol, the sensitizers themselves can resensitize ROS generation, providing they are not destroyed by the high levels of ROS.

Acknowledgements

The authors acknowledge the salary support of both the Institute of Fluorescence, IoF, and the Department of Chemistry and Biochemistry, UMBC, USA.

References

- C. D. Geddes and J. R. Lakowicz, *J. Fluoresc.*, 2002, **12**, 121–129.
- A. I. Dragan, M. T. Albrecht, R. Pavlovic, A. M. Keane-Myers and C. D. Geddes, *Anal. Biochem.*, 2012, **425**, 54–61.
- S. M. Tennant, Y. X. Zhang, J. E. Galen, C. D. Geddes and M. M. Levine, *PLoS One*, 2011, **6**, e18700.
- Y. X. Zhang, P. Agreda, S. Kelley, C. Gaydos and C. D. Geddes, *IEEE Trans. Biomed. Eng.*, 2011, **58**, 781–784.
- A. I. Dragan, K. Golberg, A. Elbaz, R. Marks, Y. X. Zhang and C. D. Geddes, *J. Immunol. Methods*, 2011, **366**, 1–7.
- A. I. Dragan, E. S. Bishop, J. R. Casas-Finet, R. J. Strouse, M. A. Schenerman and C. D. Geddes, *J. Immunol. Methods*, 2010, **362**, 95–100.
- Y. X. Zhang, K. Aslan, M. J. R. Previte, S. N. Malyn and C. D. Geddes, *J. Phys. Chem. B*, 2006, **110**, 25108–25114.
- Y. Zhang, K. Aslan, M. J. R. Previte and C. D. Geddes, *Chem. Phys. Lett.*, 2008, **458**, 147–151.
- Y. Zhang, K. Aslan, M. J. R. Previte and C. D. Geddes, *Appl. Phys. Lett.*, 2008, **92**, 013905.
- Y. X. Zhang, K. Aslan, M. J. R. Previte and C. D. Geddes, *Appl. Phys. Lett.*, 2007, **91**, 023114.
- Y. X. Zhang, K. Aslan, M. J. R. Previte and C. D. Geddes, *Biophys. J.*, 2007, 519A.
- Y. X. Zhang, K. Aslan, M. J. R. Previte and C. D. Geddes, *J. Fluoresc.*, 2007, **17**, 345–349.
- Y. Zhang, K. Aslan, M. J. R. Previte and C. D. Geddes, *Proc. Natl. Acad. Sci. U. S. A.*, 2008, **105**, 1798–1802.
- A. I. Dragan and C. D. Geddes, *Phys. Chem. Chem. Phys.*, 2011, **13**, 3831–3838.
- J. O. Karolin and C. D. Geddes, *J. Fluoresc.*, 2012, **22**, 1659–1662.
- A. Gollmer, J. Arnbjerg, F. H. Blaikie, B. W. Pedersen, T. Breitenbach, K. Daasbjerg, M. Glasius and P. R. Ogilby, *Photochem. Photobiol.*, 2011, **87**, 671–679.
- X. Ragas, A. Jimenez-Banzo, D. Sanchez-Garcia, X. Batllori and S. Nonell, *Chem. Commun.*, 2009, 2920–2922.

- 18 B. Fink, K. Laude, L. McCann, A. Doughan, D. G. Harrison and S. Dikalov, *Am. J. Physiol.: Cell Physiol.*, 2004, **287**, C895–C902.
- 19 K. M. Robinson, M. S. Janes, M. Pehar, J. S. Monette, M. F. Ross, T. M. Hagen, M. P. Murphy and J. S. Beckman, *Proc. Natl. Acad. Sci. U. S. A.*, 2006, **103**, 15038–15043.
- 20 J. Zielonka, J. Vasquez-Vivar and B. Kalyanaraman, *Nat. Protocols*, 2008, **3**, 8–21.
- 21 D. C. Fernandes, J. Wosniak, L. A. Pescatore, M. A. Bertoline, M. Liberman, F. R. M. Laurindo and C. X. C. Santos, *Am. J. Physiol.: Cell Physiol.*, 2007, **292**, C413–C422.
- 22 J. Zielonka and B. Kalyanaraman, *Free Radicals Biol. Med.*, 2010, **48**, 983–1001.
- 23 J. Zielonka, H. T. Zhao, Y. K. Xu and B. Kalyanaraman, *Free Radicals Biol. Med.*, 2005, **39**, 853–863.
- 24 H. T. Zhao, J. Joseph, H. M. Fales, E. A. Sokoloski, R. L. Levine, J. Vasquez-Vivar and B. Kalyanaraman, *Proc. Natl. Acad. Sci. U. S. A.*, 2005, **102**, 5727–5732.
- 25 K. Aslan and C. D. Geddes, *Anal. Chem.*, 2009, **81**, 6913–6922.
- 26 K. Aslan, J. Huang, G. M. Wilson and C. D. Geddes, *J. Am. Chem. Soc.*, 2006, **128**, 4206–4207.
- 27 K. Aslan, P. Holley and C. D. Geddes, *J. Immunol. Methods*, 2006, **312**, 137–147.
- 28 K. Aslan and C. D. Geddes, *Plasmonics*, 2009, **4**, 267–272.
- 29 R. Pribik, A. I. Dragan, Y. Zhang, C. Gaydos and C. D. Geddes, *Chem. Phys. Lett.*, 2009, **478**, 70–74.
- 30 D. D. Evanoff and G. Chumanov, *J. Phys. Chem. B*, 2004, **108**, 13957–13962.
- 31 A. I. Dragan, B. Mali and C. D. Geddes, *Chem. Phys. Lett.*, 2013, **556**, 168–172.
- 32 A. I. Dragan and C. D. Geddes, *Appl. Phys. Lett.*, 2012, **100**, 093115.
- 33 D. Faccio, P. Di Trapani, E. Borsella, F. Gonella, P. Mazzoldi and A. M. Malvezzi, *Europhys. Lett.*, 1998, **43**, 213–218.
- 34 K. Uchida, S. Kaneko, S. Omi, C. Hata, H. Tanji, Y. Asahara, A. J. Ikushima, T. Tokizaki and A. Nakamura, *J. Opt. Soc. Am. B*, 1994, **11**, 1236–1243.